Supplementary Information

Synaptotagmin 1 oligomers clamp and regulate different modes of neurotransmitter release.

Erica Tagliatti, Oscar D. Bello, Philipe R. F. Mendonça, Dimitrios Kotzadimitriou, Elizabeth Nicholson, Jeff Coleman, Yulia Timofeeva, James E. Rothman, Shyam S. Krishnakumar* and Kirill E. Volynski*.

*To whom correspondence may be addressed. Email: k.volynski@ucl.ac.uk or s.krishnakumar@ucl.ac.uk

This PDF file includes:

      Supplementary Discussion
      Figures S1 to S6
      Table S1

Supplementary Discussion

Comparison of the RRP sizes in Syt1^{-/-} and Syt1^{+/+} neurons

Functional definition of RRP

In most general terms, the RRP of vesicles is functionally defined as a small subset of vesicles in the presynaptic terminal that can be released by Ca^{2+} or hyperosmotic stimulation on a faster time scale than the other vesicles in the terminal (9, 12). It is thought that most of the RRP vesicles correspond to the vesicles that are morphologically docked and primed for release at the presynaptic active zone. The priming process includes the formation of partially-assembled SNARE complexes, which are arrested in this state by synaptotagmin and complexin molecules (13, 14). However, not all of the docked vesicles necessarily belong to the RRP, and in some cases undocked vesicles can also contribute to the RRP (6).

Different methods to measure RRP size

A detailed comparison of methods used to measure RRP size is outlined in the recent review by Kaiser and Regehr (6). Briefly, there are three major ways of estimating RRP size, that are based on (i) electrophysiological measurements of evoked post-synaptic currents, (ii) recordings of presynaptic capacitance, and (iii) fluorescent imaging of vesicular release at presynaptic terminals. Each of these approaches has its advantages and limitations. The major challenge that is common for all three techniques is to find a stimulus that can quickly release the entire RRP but minimise overestimation of the RRP size due to synaptic vesicle replenishment.

Estimation of relative RRP size using pHluorin imaging approach used in our study

To estimate the RRP size, we adapted the approach developed by Ariel and Ryan, which is based on imaging of sypHy (or vGlut-pHluorin) fluorescence transients evoked by a short (20 APs) high frequency (100 Hz) burst of stimulation (1). Such stimulation paradigm produces brief but sufficiently large presynaptic $[Ca^{2+}]$ transient that triggers release of most RRP vesicles on a time scale of 200 ms. Importantly, it has been demonstrated that synaptic vesicle replenishment does not significantly contributes to the RRP estimate on this time scale (1).

Here we have further validated the Ariel and Ryan paradigm. We performed a control experiment with Bafilomycin treatment, which demonstrated that synaptic vesicle endocytosis does not contribute to our estimates of relative RRP size in both Syt1^{-/-} and Syt1^{+/+} neurons (Fig. S3). This result is in line with the recent findings, which demonstrate that compensatory endocytosis triggered by high-frequency bursts of APs mainly occurs on the time scale of several seconds (*e.g.* Fig.1 in ref. (11)). In contrast, compensatory endocytosis triggered by single spikes predominantly occurs on a time scale of hundreds of milliseconds (3, 15).

pHluorin-based approach does not distinguish between synchronous and asynchronous release that occurs in-between spikes of the 20 AP 100 Hz train, but instead measures cumulative total release. This is conceptually similar to the electrophysiological measurements of cumulative charge transfer during AP-bursts (12). The importance of cumulative measurements of both synchronous and asynchronous release components when estimating RRP with AP bursts has been emphasised earlier (12), and this becomes particularly essential when estimating RRP size in Syt1^{-/-} neurons, which is predominantly asynchronous (5). Comparison of sypHy responses in Syt1^{+/+} and Syt1^{-/-} neurons during 20 AP 100 Hz burst (recorded with 50 ms resolution) revealed similar sypHy kinetics, which plateaued by the end of the stimulation in both genotypes. This result is consistent with electrophysiological recordings in the Calyx of Held, which show that in the absence of Syt1/Syt2 RRP can still be discharged by presynaptic depolarisation on a time-scale of 200 -300 ms (*e.g.* Fig. 7 in ref. (7)).

Comparison of RRP size in Syt1^{-/-} and Syt1^{+/+} neurons.

There have been conflicting data on how genetic deletion of Syt1 affects the RRP size. On the one hand several groups have reported ~ 25 - 50 % reduction in the RRP size measured using sucrose stimulation in neuronal cultures (*e.g.* refs. (4, 8)). On the other hand, other groups using the same technique did not find significant differences in the RRP between Syt1^{-/-} and Syt1^{+/+} neurons (5, 16), and have in fact suggested that Syt1 and Syt7 are redundantly required for RRP maintenance (2).

It is likely that the observed discrepancies could be due to distinct effects of Syt1 KO on RRP in different types of synapses (*e.g.* excitatory versus inhibitory) or due to differences in neuronal culture preparations used by different groups (*e.g.* type of culture, neuronal density).

Our sypHy imaging experiments indicate that RRP size was not affected by Syt1 KO in our preparation. To test this further we estimated RRP size by 0.5 M sucrose stimulation (Fig. S4) using the established protocol (4, 9). We found a small (~ 20%) decrease in sucrose-induced postsynaptic excitatory responses in Syt1$^{-/-}$ neurons. Interestingly, we also observed a comparable decrease in neuronal capacitance, which is directly related to the neuronal size and therefore to the number of synapses formed on the recorded postsynaptic neuron. When normalised to the cell capacitance, the sucrose-induced responses were similar in Syt1$^{-/-}$ and Syt1$^{+/+}$ neurons. This indicates that in our experimental conditions Syt1 KO does not affect RRP size, measured with sucrose stimulation at the level of individual synapses, which is in full agreement with the sypHy RRP estimates (Fig. 2 and Fig. S3). In line with the reduction of overall neuronal size, as indicated by the capacitance measurements, Sholl analysis of dendritic morphology revealed a significant reduction of neuronal arborisation in Syt1$^{-/-}$ cortical neurons. This decrease of dendritic arborisation in Syt1$^{-/-}$ neurons is possibly caused by homeostatic compensatory mechanisms. Indeed, it is likely that deletion of Syt1, which results in near complete abolishment of synchronous neurotransmitter release, will affect neuronal network activity and invoke homeostatic changes. Thus, our findings call attention to the importance of accounting for such mechanisms when estimating effect of Syt1 KO on RRP size and other synaptic functional properties.
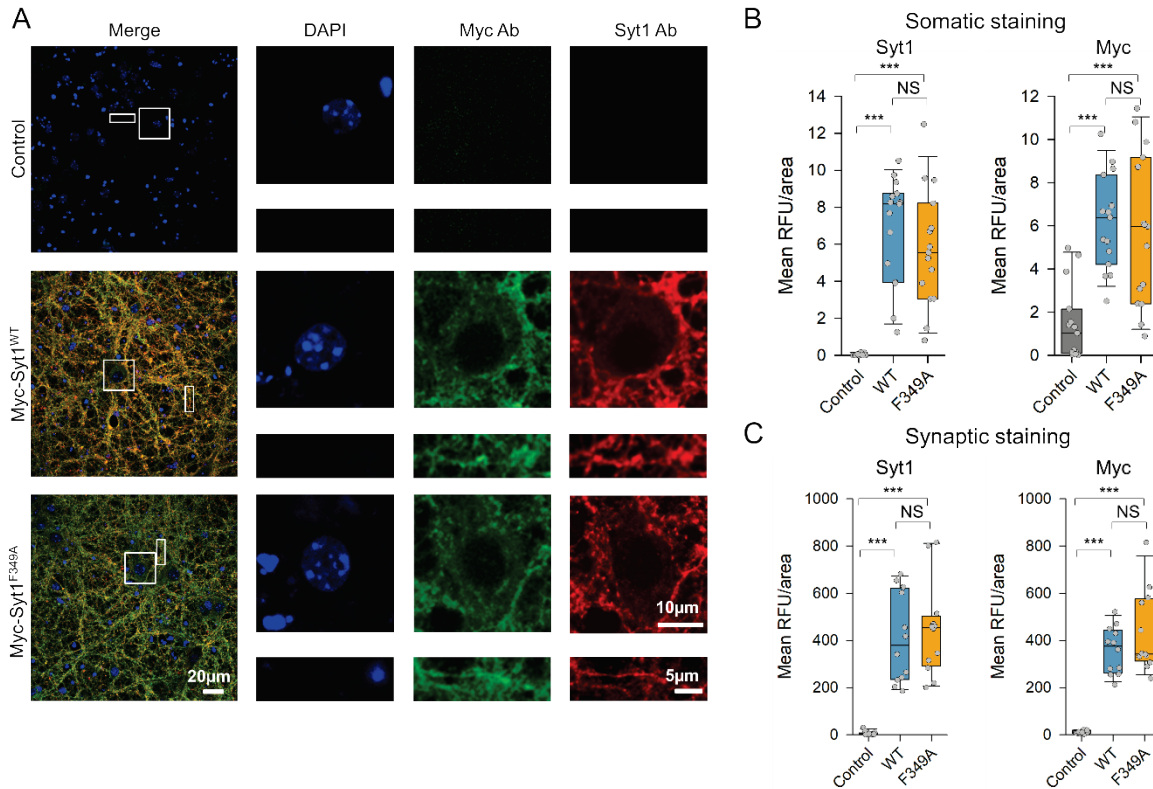
Figure S1. Overexpression of Myc-Syt1^{WT} and Myc-Syt1^{F349A} in Syt1^{-/-} neurons.

(A) Representative images of untransduced Syt1$^{-/-}$ neurons (Control) and of Syt1$^{-/-}$ neurons transduced either with Myc-Syt1^{WT} or Myc-Syt1^{F349A} lentiviruses immunostained with Abs against Myc tag (green) and Syt1 (red). DAPI was used to visualise the cell nuclei. Two different types of ROIs (right panels and corresponding white boxes on the original images) containing either somas or neurites were used to quantify somatic and synaptic Myc and Syt1 immunoreactivity respectively. Transduction efficiency was in the range of 80 − 95%. (B, C) Quantification of somatic and synaptic Myc and Syt1 immunofluorescence levels showing rescue of Syt1 expression in the transduced neurons. *** p < 0.001, NS p > 0.3, Mann–Whitney U test. The detailed statistical analysis is reported in Table S1.
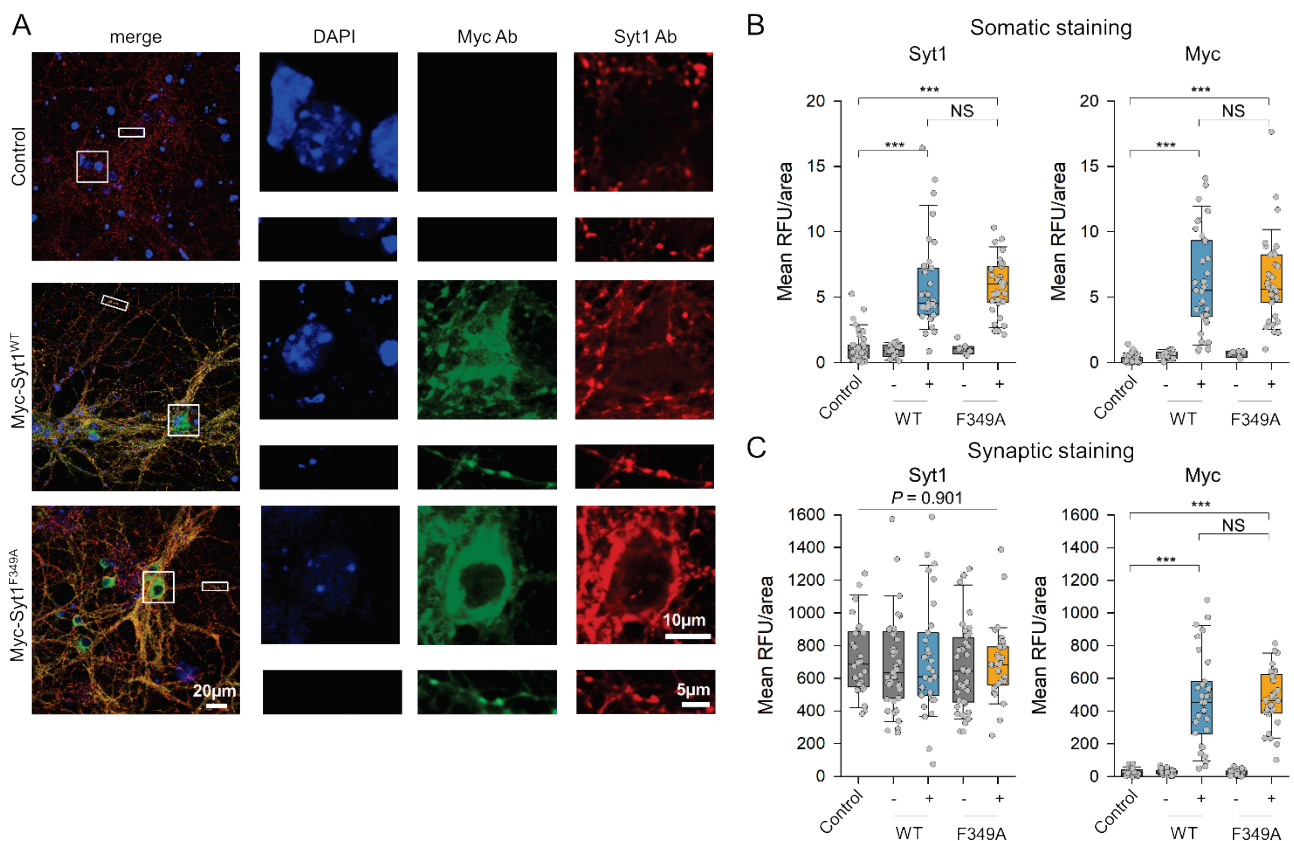
Figure S2. Overexpression of Myc-Syt1^{WT} and Myc-Syt1^{F349A} in Syt1$^{+/+}$ neurons.

(A) Representative images of untransduced Syt1$^{+/+}$ neurons (Control) and of Syt1$^{+/+}$ neurons transduced either with Myc-Syt1^{WT} or Myc-Syt1^{F349A} lentiviruses immunostained with Abs against Myc tag (green) and Syt1 (red). DAPI was used to visualise the cell nuclei. Two different types of ROIs (right panels and corresponding white boxes on the original images) containing either somas or neurites were used to quantify somatic and synaptic Myc and Syt1 immunoreactivity respectively. Transduction efficiency was > 90 – 95 %

(B, C) Quantification of somatic and synaptic Myc and Syt1 immunofluorescence levels showing increase of Syt1 expression in somatic but not synaptic areas of the transduced neurons. An additional internal control was added in this set of experiments (WT (-) and F349A (-)), where untransduced myc-negative cells, expressing endogenous Syt1 only, were analysed in parallel when present in the same field of view. *** p < 0.001, NS p > 0.5, Mann–Whitney U test. The detailed statistical analysis is reported in Table S1.
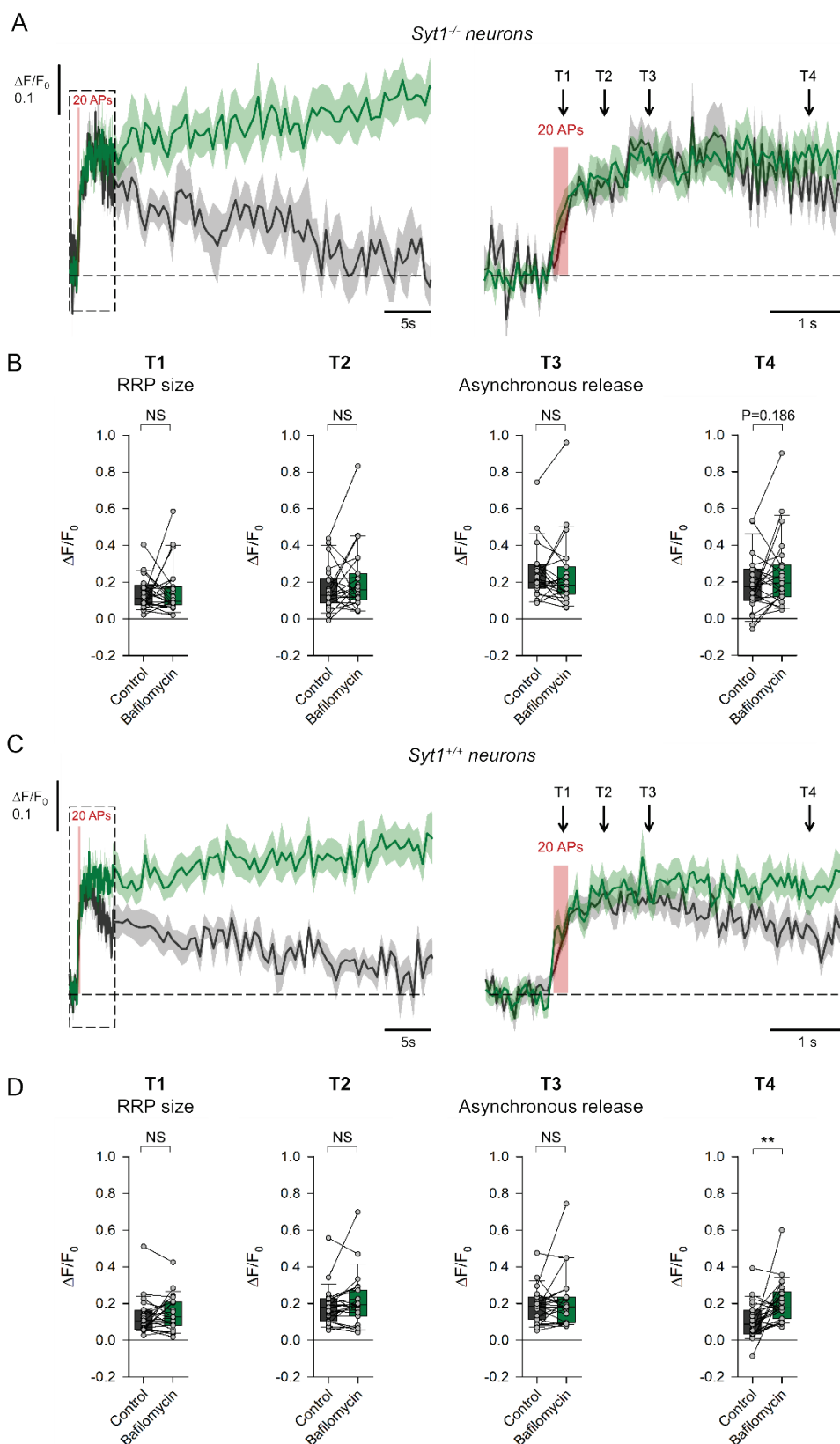
Figure S3. Bafilomycin re-acidification block demonstrates that endocytosis does not affect sypHy-based measurements of the RRP size and the delayed asynchronous release after the burst.

(A, C) Left, average sypHy fluorescence traces in response to 20 AP 100Hz stimulation recorded in Syt1$^{-/-}$ (A) and Syt1$^{+/+}$ (C) neurons before (grey) and after (green) application of 1 μM Bafilomycin (n = 23 coverslips for each condition, shaded areas represent SEM). The first 5 seconds (dashed boxes) were recorded at 20 Hz frame rate, the rest of the data (between 5 – 40 seconds) were collected at 2 Hz frame rate to minimise photobleaching. Right, zoomed view of the first 5 seconds of the recordings. Due to endocytosis and synaptic

vesicle re-acidification sypHy responses in the absence of Bafilomycin decay on a time-scale of tens of seconds in both Syt1$^{-/-}$ and Syt1$^{+/+}$ neurons (left). Importantly, endocytosis has minimal contribution to sypHy transients within ~ 1.5 sec after the burst, as they are similar before and after Bafilomycin treatment.

(B, D) Data from individual cells showing changes of $\Delta F/F_0$ sypHy responses before and after application of Bafilomycin at the indicated time points T1, T2, T3 and T4 (arrows on the traces above). This experiment demonstrates that endocytosis and synaptic re-acidification has minimal contribution to the estimates of the relative RRP size (performed immediately after the AP burst) and the delayed asynchronous release component (average of 8 frames within 0.9 – 1.25 sec after the burst, T3). NS p > 0.2, Paired t-test on Ranks. The detailed statistical analysis including the numbers of independent experiments is reported in Table S1. See also Supplementary Discussion on comparison of RRP sizes in Syt1$^{-/-}$ and Syt1$^{+/+}$ neurons.
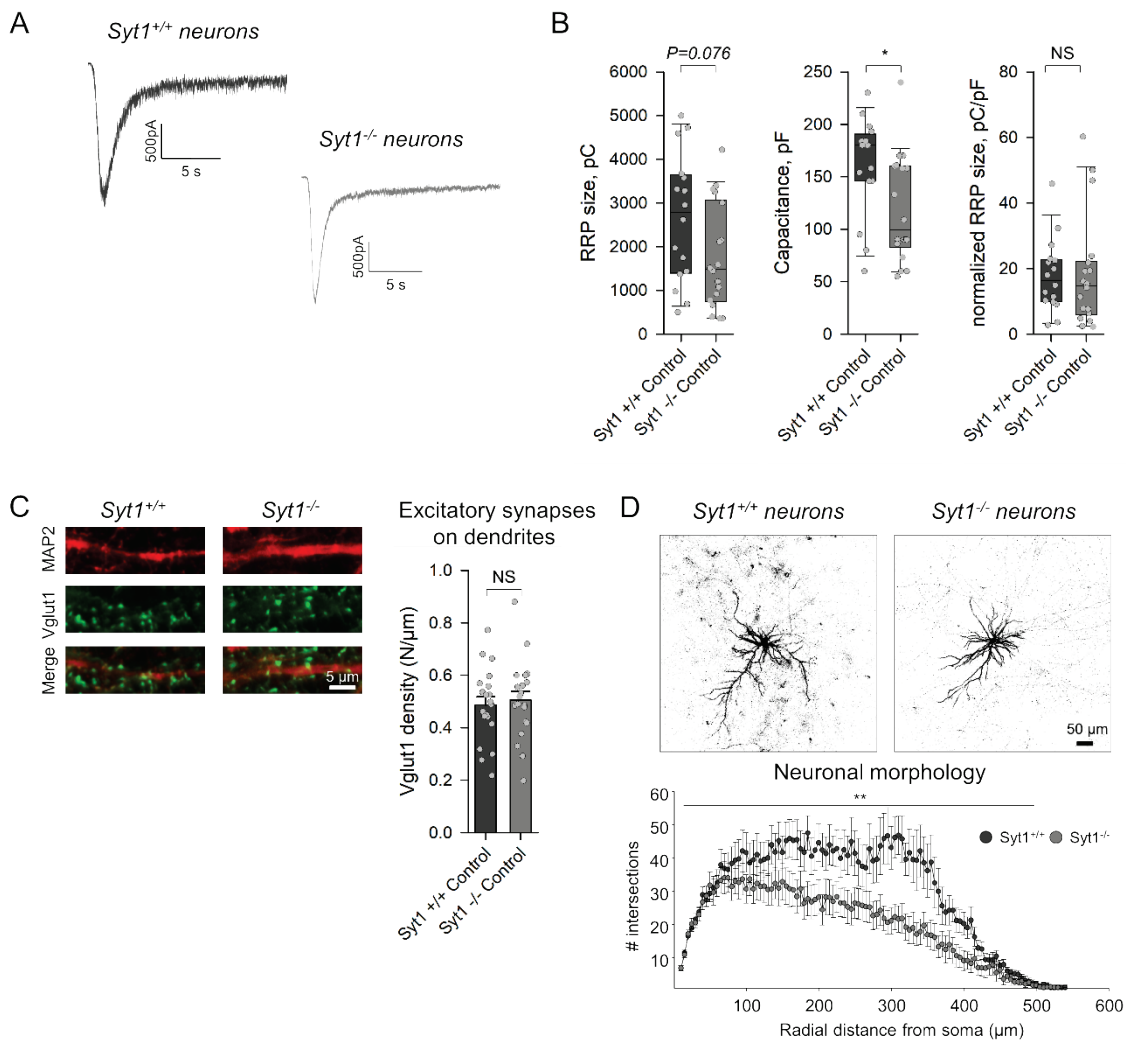
Figure S4. RRP size estimated with transient hyperosmotic sucrose stimulation is similar in Syt1$^{-/-}$ and Syt1$^{+/+}$ neuronal synapses.

(A) Representative traces of postsynaptic response induced by 15 s application of 0.5 M Sucrose used to estimate RRP size in Syt1$^{+/+}$ and Syt1$^{-/-}$ neurons.

(B) Summary box-and-dot plots of RRP size, membrane capacitance and normalised RRP size. Small decrease of sucrose-induced response in Syt1$^{-/-}$ neurons can be explained by the concurrent decrease of neuronal capacitance, which is directly related to the neuronal membrane size. When normalised to cell capacitance sucrose-induced responses were similar in Syt1$^{-/-}$ and Syt1$^{+/+}$ neurons indicating that Syt1 KO does not affect RRP size in individual synapses, which is in full agreement with sypHy measurements in Fig.2 and Fig. S3. *p < 0.05, NS p > 0.5. Mann–Whitney U test.

(C) Density of glutamatergic synapses is not changed in Syt1 KO. Left, representative images of dendritic branches from Syt1$^{+/+}$ and Syt1$^{-/-}$ neurons immunostained with Abs against Map2 (red) and VGlut1 (green). Right, quantification bar plots, where synaptic density expressed as a number of VGlut1 positive boutons per µm of dendritic branch length. NS p > 0.5. Student t-test.

(D) Sholl analysis of dendritic morphology (visualised with iGluSnFR expression) reveals an overall reduction of neuronal arborisation in Syt1$^{-/-}$ cortical neurons, in line with the overall reduction of neuronal size as established with capacitance measurements in (B). **p < 0.01. Two-way ANOVA on Ranks. The detailed statistical analysis including the numbers of independent experiments is reported in Table S1.
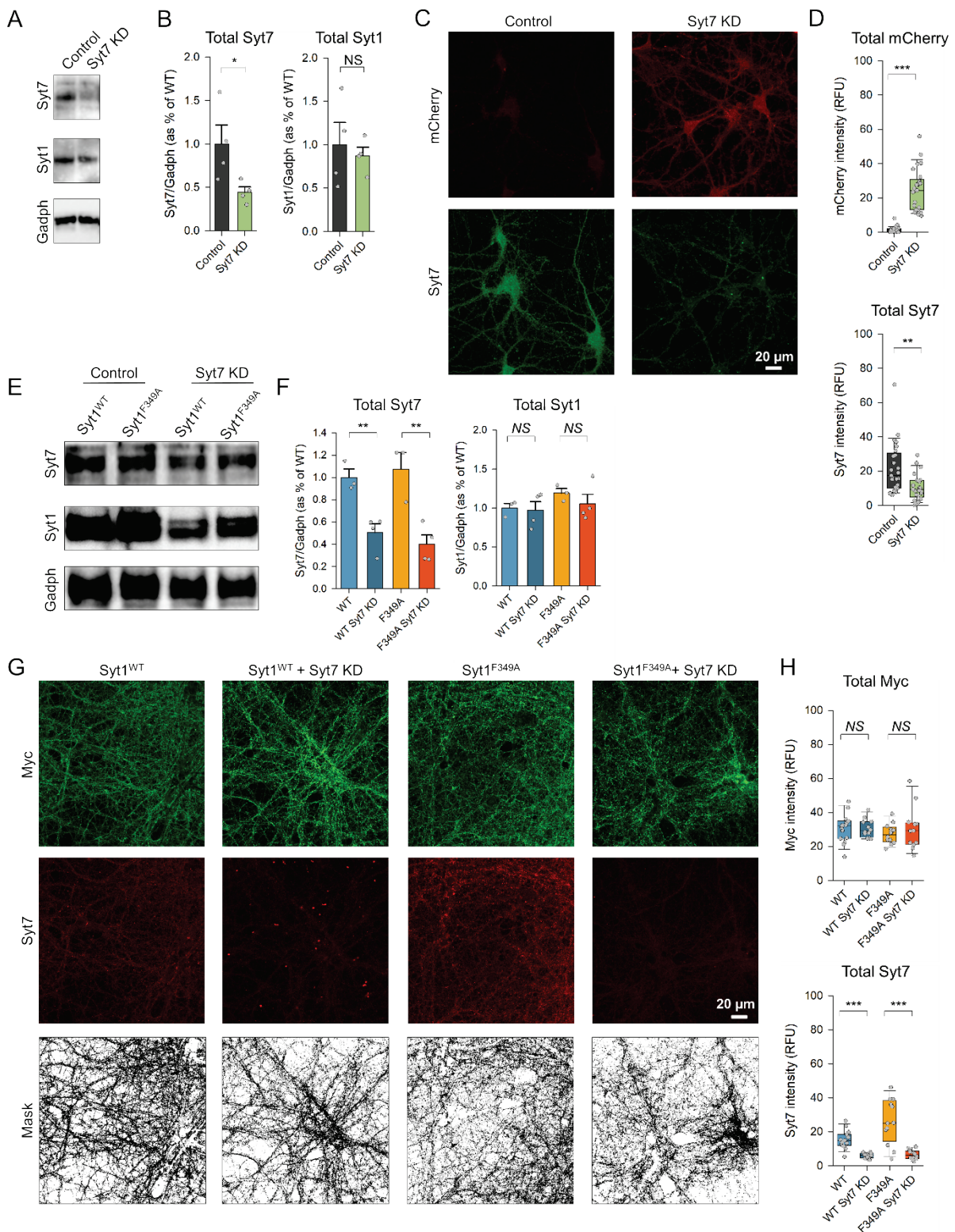
Figure S5. Syt7 Knock Down (KD) wild type neurons using mono and bi-cystronic lentiviruses.

(A) Representative Western Blot analysis of Syt7 and Syt1 protein levels in cell lysates from Syt1^{+/+} untransduced neurons (Control) and neurons transduced with Syt7 KD lentivirus construct.

(B) Quantification of Syt7 and Syt1 protein levels normalised to the Gadph loading control.

(C) Representative images of control neurons and neurons transduced with Syt7 KD lentivirus construct immunostained with Ab against Syt7 (green). mCherry fluorescence was used to control the transduction efficiency.

(D) Quantification of total mCherry and Syt7 fluorescence reveals a significant decrease of Syt7 levels upon Syt7 KD.

(E) Representative Western Blot analysis of Syt7 and Syt1 protein levels in cell lysates from Syt1$^{+/+}$ neurons transduced with Myc-Syt1^{WT}, Myc-Syt1^{F349A}, Myc-Syt^{WT}-Syt7-KD or Myc-Syt1^{F349A}-Syt7-KD lentiviral constructs.

(F) Quantification of Syt7 and Syt1 protein levels normalised to the Gadph loading control.

(G) Representative images of Syt1$^{+/+}$ neurons transduced with Myc-Syt1^{WT}, Myc-Syt1^{F349A}, Myc-Syt^{WT}-Syt7-KD or Myc-Syt1^{F349A}-Syt7-KD lentiviral constructs, immunostained with Abs against Myc tag (green) and Syt7 (red). A binary mask created from the Myc image was applied to estimate the relative Syt7 immunoreactivity.

(H) Quantification of total Myc and Syt7 fluorescence reveals a significant decrease of Syt7 levels in Syt7 KD neurons compared to the relative controls.

* $p < 0.05$, ** $p < 0.01$, *** $p < 0.001$, NS $p > 0.4$, Student t-test (B and F), Mann–Whitney U test (D and H). The detailed statistical analysis is reported in Table S1.
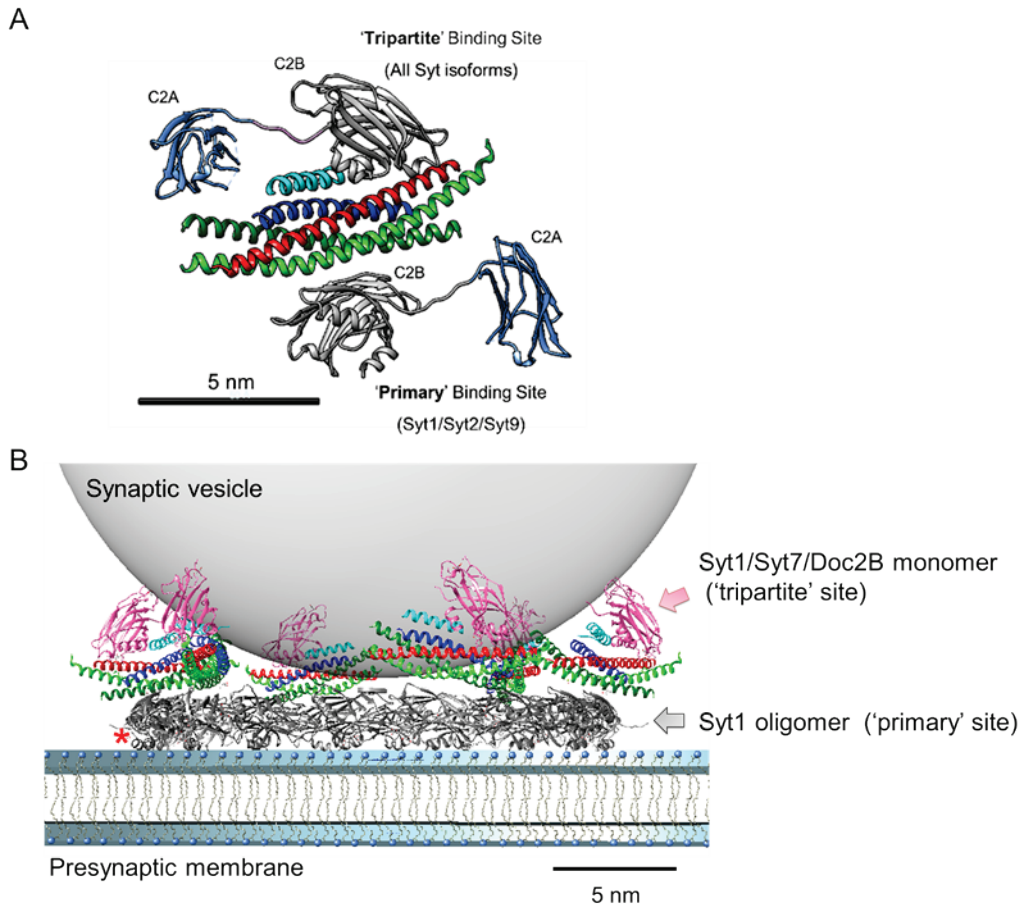
Figure S6. Molecular model for the clamping of vesicular fusion by Syt1 ring-like oligomers.

This model, combining the recent X-ray SNAREpin-Syt1-complexin structure (17) with the molecular architecture of Syt1 ring-like oligomers, could potentially explain the Syt1 clamping function in molecular terms (10). (A) The X-ray crystal structure shows that each pre-fusion partially assembled SNARE complex (SNAREpin) contains two distinct Syt1 binding sites: a complexin-independent 'primary' site, which can only be occupied by synaptotagmins that mediate synchronous release (Syt1, Syt2 and Syt9) and a complexin-dependent 'tripartite' site which is potentially available to all synaptotagmin isoforms, including Syt7 (17).

(B) We posit that the full complement (15-20 copies) of Syt1 on the vesicle oligomerise at the site of docking triggered by PIP2 binding. This Syt1 oligomer (grey) is then ideally positioned to simultaneously template multiple SNAREpins via the 'primary' binding motif, which is accessible and free to interact in the ring oligomer. Note that in the ring-oligomer configuration, the conserved helical extension (red asterisk) involved in the tripartite binding locates towards the membrane and is thus unavailable. The height of Syt1 oligomers combined with the SNAREs atop would maintain the two bilayers far apart (~4 nm) to allow the N-terminal assembly but to sterically block the complete assembly of SNAREs. Furthermore, Syt1 oligomers are also expected to restrain the bound SNAREpins from moving inward toward the incipient fusion pore. Thus, the ring oligomer will clamp the synaptic vesicle fusion. In this arrangement, a second independent C2B domain (magenta) from either Syt1, Syt7 or Doc2B (17) can bind the SNAREpin via the 'tripartite' site in conjunction with complexin (cyan) and further, stabilise the fusion clamp. Upon Ca^{2+} influx, the Syt1 ring oligomers are disrupted as Syt1 molecules rotate to insert into the plasma membrane. This frees the SNAREpins to complete zippering and trigger fusion. In this manner, the Syt1 oligomer could mediate a Ca^{2+}-sensitive clamp on vesicular fusion. Critically, this dual-clamp model illustrates how Syt1 oligomerization could gate activation of both Syt1 and the second Ca^{2+} sensor (e.g. Syt7). Adapted from refs. (10, 17).

Table S1 **Statistical Analysis**

<u>**Figure 1**</u>

Condition	Number of preparations
Syt1^{WT}	3
Syt1^{F349A}	3
Syt1^{F349A} + Syt1^{WT} 1:2	3
Syt1^{F349A} + Syt1^{WT} 1:1	3
Syt1^{F349A} + Syt1^{WT} 2:1	3

Figure 1D Total oligomeric structures

Condition 1	Condition 2	P value	Statistical test
Syt1^{WT}	Syt1^{F349A}	P < 0.001	Student t-test
Syt1^{WT}	Syt1^{F349A} + Syt1^{WT}, 1:2	P = 0.153	Student t-test
Syt1^{WT}	Syt1^{F349A} + Syt1^{WT}, 1:1	P = 0.020	Student t-test
Syt1^{WT}	Syt1^{F349A} + Syt1^{WT}, 2:1	P < 0.001	Student t-test
Syt1^{F349A}	Syt1^{F349A} + Syt1^{WT}, 1:2	P < 0.001	Student t-test
Syt1^{F349A}	Syt1^{F349A} + Syt1^{WT}, 1:1	P < 0.001	Student t-test
Syt1 ^{F349A}	Syt1^{F349A} + Syt1^{WT}, 2:1	P < 0.001	Student t-test

Figure 1D Ring-like oligomeric structures

Condition 1	Condition 2	P value	Statistical test
Syt1^{WT}	Syt1^{F349A}	P < 0.001	Student t-test
Syt1^{WT}	Syt1^{F349A} + Syt1^{WT}, 1:2	P = 0.002	Student t-test
Syt1^{WT}	Syt1^{F349A} + Syt1^{WT}, 1:1	P < 0.001	Student t-test
Syt1^{WT}	Syt1^{F349A} + Syt1^{WT}, 2:1	P < 0.001	Student t-test
Syt1^{F349A}	Syt1^{F349A} + Syt1^{WT}, 1:2	P < 0.001	Student t-test
Syt1^{F349A}	Syt1^{F349A} + Syt1^{WT}, 1:1	P = 0.048	Student t-test
Syt1 ^{F349A}	Syt1^{F349A} + Syt1^{WT}, 2:1	P < 0.001	Student t-test

Figure 1E Oligomeric rings diameter

Condition 1	Condition 2	P value	Statistical test
Syt1^{WT}	Syt1^{F349A}	P = 0.196	Student t-test
Syt1^{WT}	Syt1^{F349A} + Syt1^{WT}, 1:2	P = 0.002	Student t-test
Syt1^{WT}	Syt1^{F349A} + Syt1^{WT}, 1:1	P = 0.002	Student t-test
Syt1^{WT}	Syt1^{F349A} + Syt1^{WT}, 2:1	P < 0.001	Student t-test
Syt1^{F349A}	Syt1^{F349A} + Syt1^{WT}, 1:2	P = 0.018	Student t-test
Syt1^{F349A}	Syt1^{F349A} + Syt1^{WT}, 1:1	P < 0.001	Student t-test
Syt1 ^{F349A}	Syt1^{F349A} + Syt1^{WT}, 2:1	P < 0.001	Student t-test

Figure 1E Cumulative probability

Condition	Number of ring-like particles
Syt1^{WT}	365
Syt1^{F349A}	53

Syt1^{F349A} + Syt1^{WT} 1:2	287	
Syt1^{F349A} + Syt1^{WT} 1:1	200	
Syt1^{F349A} + Syt1^{WT} 2:1	201	

Figure 2

Condition	Number of imaged coverslips	Number of culture preparations
Syt1$^{-/-}$ Control	12	6
Syt1$^{-/-}$ Syt1^{WT}	15	7
Syt1$^{-/-}$ Syt1^{F349A}	15	7
Syt1$^{+/+}$ Control	29	9
Syt1$^{+/+}$ Syt1^{WT}	23	9
Syt1$^{+/+}$ Syt1^{F349A}	25	10
Syt1$^{+/+}$ Syt7 KD only	27	6
Syt1$^{+/+}$ Syt1^{WT} Syt7 KD	24	10
Syt1$^{+/+}$ Syt1^{F349A} Syt7 KD	28	11

Figure 2B

Syt1$^{-/-}$ background, one way ANOVA on ranks $P = 0.981$

Syt1$^{+/+}$ background, one way ANOVA on ranks $P = 0.968$

Syt1$^{+/+}$ background + Syt7 KD, one way ANOVA on ranks $P = 0.172$

Figure 2C

Condition 1	Condition 2	P value	Statistical test
Syt1$^{-/-}$ Control	Syt1$^{-/-}$ Syt1^{WT}	P < 0.001	Mann-Whitney U test
Syt1$^{-/-}$ Control	Syt1$^{-/-}$ Syt1^{F349A}	P < 0.001	Mann-Whitney U test
Syt1$^{-/-}$ Syt1^{WT}	Syt1$^{-/-}$ Syt1^{F349A}	P < 0.001	Mann-Whitney U test
Syt1$^{+/+}$ Control	Syt1$^{+/+}$ Syt1^{WT}	P = 0.439	Mann-Whitney U test
Syt1$^{+/+}$ Control	Syt1$^{+/+}$ Syt1^{F349A}	P < 0.001	Mann-Whitney U test
Syt1$^{+/+}$ Syt1^{WT}	Syt1$^{+/+}$ Syt1^{F349A}	P < 0.001	Mann-Whitney U test
Syt1$^{+/+}$ Syt7 KD only	Syt1$^{+/+}$ Syt1^{WT} Syt7 KD	P = 0.058	Mann-Whitney U test
Syt1$^{+/+}$ Syt7 KD only	Syt1$^{+/+}$ Syt1^{F349A} Syt7 KD	P < 0.001	Mann-Whitney U test
Syt1$^{+/+}$ Syt1^{WT} Syt7 KD	Syt1$^{+/+}$ Syt1^{F349A} Syt7 KD	P = 0.007	Mann-Whitney U test

Figure 2D

Syt1$^{+/+}$ background + Syt7 KD, one way ANOVA on ranks $P = 0.791$

Condition 1	Condition 2	P value	Statistical test
Syt1$^{-/-}$ Control	Syt1$^{-/-}$ Syt1^{WT}	P = 0.020	Mann-Whitney U test
Syt1$^{-/-}$ Control	Syt1$^{-/-}$ Syt1^{F349A}	P = 0.608	Mann-Whitney U test
Syt1$^{-/-}$ Syt1^{WT}	Syt1$^{-/-}$ Syt1^{F349A}	P = 0.020	Mann-Whitney U test
Syt1$^{+/+}$ Control	Syt1$^{+/+}$ Syt1^{WT}	P = 0.699	Mann-Whitney U test
Syt1$^{+/+}$ Control	Syt1$^{+/+}$ Syt1^{F349A}	P < 0.001	Mann-Whitney U test
Syt1$^{+/+}$ Syt1^{WT}	Syt1$^{+/+}$ Syt1^{F349A}	P = 0.003	Mann-Whitney U test
Syt1$^{+/+}$ Syt7 KD only	Syt1$^{+/+}$ Syt1^{WT} Syt7 KD	P = 0.578	Mann-Whitney U test
Syt1$^{+/+}$ Syt7 KD only	Syt1$^{+/+}$ Syt1^{F349A} Syt7 KD	P = 0.926	Mann-Whitney U test

Syt1$^{+/+}$ Syt1^{WT} Syt7 KD	Syt1$^{+/+}$ Syt1^{F349A} Syt7 KD	P = 0.539	Mann-Whitney U test

Figure 3

Condition	Number of cells	Number of preparations
Syt1$^{+/+}$ Syt1^{WT}	17	7
Syt1$^{+/+}$ Syt1^{F349A}	17	7

Figure 3C Synchronous release

Condition 1	Condition 2	P value	Statistical test
Syt1$^{+/+}$ Syt1^{WT} 1st AP	Syt1$^{+/+}$ Syt1^{F349A} 1st AP	P = 0.121	Mann-Whitney U test
Syt1$^{+/+}$ Syt1^{WT} last 20 APs	Syt1$^{+/+}$ Syt1^{F349A} last 20 APs	P = 0.605	Mann-Whitney U test

Figure 3C Asynchronous release

Condition 1	Condition 2	P value	Statistical test
Syt1$^{+/+}$ Syt1^{WT} 1st AP	Syt1$^{+/+}$ Syt1^{F349A} 1st AP	P = 0.585	Mann-Whitney U test
Syt1$^{+/+}$ Syt1^{WT} last 20 APs	Syt1$^{+/+}$ Syt1^{F349A} last 20 APs	P = 0.016	Mann-Whitney U test

Figure 4

Condition	Number of cells	Number of preparations
Syt1$^{-/-}$ Control	25	4
Syt1$^{-/-}$ Syt1^{WT}	20	5
Syt1$^{-/-}$ Syt1^{F349A}	30	7
Syt1$^{+/+}$ Control	21	5
Syt1$^{+/+}$ Syt1^{WT}	21	5
Syt1$^{+/+}$ Syt1^{F349A}	19	5

Figure 4B

Condition 1	Condition 2	P value	Statistical test
Syt1$^{-/-}$ Control	Syt1$^{-/-}$ Syt1^{WT}	P < 0.001	Mann-Whitney U test
Syt1$^{-/-}$ Control	Syt1$^{-/-}$ Syt1^{F349A}	P = 0.240	Mann-Whitney U test
Syt1$^{-/-}$ Syt1^{WT}	Syt1$^{-/-}$ Syt1^{F349A}	P = 0.012	Mann-Whitney U test
Syt1$^{+/+}$ Control	Syt1$^{+/+}$ Syt1^{WT}	P = 0.814	Mann-Whitney U test
Syt1$^{+/+}$ Control	Syt1$^{+/+}$ Syt1^{F349A}	P = 0.032	Mann-Whitney U test
Syt1$^{+/+}$ Syt1^{WT}	Syt1$^{+/+}$ Syt1^{F349A}	P = 0.021	Mann-Whitney U test

Figure 4C

Syt1$^{-/-}$ background, one way ANOVA on ranks P = 0.18

Syt1$^{+/+}$ background, one way ANOVA on ranks P = 0.17

Figure S1

Condition	Number of cell somas	Number of synaptic ROIs	Number of preparations
Syt1$^{-/-}$ Control	15	12	3
Syt1$^{-/-}$ Syt1^{WT}	15	12	3
Syt1$^{-/-}$ Syt1^{F349A}	15	12	3

Figure S1B anti-Syt1 Ab

Condition 1	Condition 2	P value	Statistical test
Syt1$^{-/-}$ Control	Syt1$^{-/-}$ Syt1^{WT}	P < 0.001	Mann-Whitney U test
Syt1$^{-/-}$ Control	Syt1$^{-/-}$ Syt1^{F349A}	P < 0.001	Mann-Whitney U test
Syt1$^{-/-}$ Syt1^{WT}	Syt1$^{-/-}$ Syt1^{F349A}	P = 0.300	Mann-Whitney U test

Figure S1B anti-Myc Ab

Condition 1	Condition 2	P value	Statistical test
Syt1$^{-/-}$ Control	Syt1$^{-/-}$ Syt1^{WT}	P < 0.001	Mann-Whitney U test
Syt1$^{-/-}$ Control	Syt1$^{-/-}$ Syt1^{F349A}	P < 0.001	Mann-Whitney U test
Syt1$^{-/-}$ Syt1^{WT}	Syt1$^{-/-}$ Syt1^{F349A}	P = 0.590	Mann-Whitney U test

Figure S1C anti-Syt1 Ab

Condition 1	Condition 2	P value	Statistical test
Syt1$^{-/-}$ Control	Syt1$^{-/-}$ Syt1^{WT}	P < 0.001	Mann-Whitney U test
Syt1$^{-/-}$ Control	Syt1$^{-/-}$ Syt1^{F349A}	P < 0.001	Mann-Whitney U test
Syt1$^{-/-}$ Syt1^{WT}	Syt1$^{-/-}$ Syt1^{F349A}	P = 0.583	Mann-Whitney U test

Figure S1C anti-Myc Ab

Condition 1	Condition 2	P value	Statistical test
Syt1$^{-/-}$ Control	Syt1$^{-/-}$ Syt1^{WT}	P < 0.001	Mann-Whitney U test
Syt1$^{-/-}$ Control	Syt1$^{-/-}$ Syt1^{F349A}	P < 0.001	Mann-Whitney U test
Syt1$^{-/-}$ Syt1^{WT}	Syt1$^{-/-}$ Syt1^{F349A}	P = 0.371	Mann-Whitney U test

Figure S2

Condition	Number of cell somas	Number of synaptic ROIs	Number of preparations
Syt1$^{+/+}$ Control	39	26	6
Syt1$^{+/+}$ Internal Control WT	14	39	5
Syt1$^{+/+}$ Internal Control F349A	7	40	6
Syt1$^{+/+}$ Syt1^{WT}	35	31	7
Syt1$^{+/+}$ Syt1^{F349A}	35	29	7

Figure S2B anti-Syt1 Ab

Condition 1	Condition 2	P value	Statistical test
Syt1$^{+/+}$ Control	Syt1$^{+/+}$ Syt1^{WT}	P < 0.001	Mann-Whitney U test
Syt1$^{+/+}$ Control	Syt1$^{+/+}$ Syt1^{F349A}	P < 0.001	Mann-Whitney U test
Syt1$^{+/+}$ Syt1^{WT}	Syt1$^{+/+}$ Syt1^{F349A}	P = 0.231	Mann-Whitney U test

Syt1$^{+/+}$ Internal Control WT	Syt1$^{+/+}$ Syt1^{WT}	P < 0.001	Mann-Whitney U test
Syt1$^{+/+}$ Internal Control F349A	Syt1$^{+/+}$ Syt1^{F349A}	P < 0.001	Mann-Whitney U test

Figure S2B anti-Myc Ab

Condition 1	Condition 2	P value	Statistical test
Syt1$^{+/+}$ Control	Syt1$^{+/+}$ Syt1^{WT}	P < 0.001	Mann-Whitney U test
Syt1$^{+/+}$ Control	Syt1$^{+/+}$ Syt1^{F349A}	P < 0.001	Mann-Whitney U test
Syt1$^{+/+}$ Syt1^{WT}	Syt1$^{+/+}$ Syt1^{F349A}	P = 0.851	Mann-Whitney U test
Syt1$^{+/+}$ Internal Control WT	Syt1$^{+/+}$ Syt1^{WT}	P < 0.001	Mann-Whitney U test
Syt1$^{+/+}$ Internal Control F349A	Syt1$^{+/+}$ Syt1^{F349A}	P < 0.001	Mann-Whitney U test

Figure S2C anti-Syt1 Ab

Condition 1	Condition 2	P value	Statistical test
Syt1$^{+/+}$ Control	Syt1$^{+/+}$ Syt1^{WT}	P = 0.570	Mann-Whitney U test
Syt1$^{+/+}$ Control	Syt1$^{+/+}$ Syt1^{F349A}	P = 0.730	Mann-Whitney U test
Syt1$^{+/+}$ Syt1^{WT}	Syt1$^{+/+}$ Syt1^{F349A}	P = 0.679	Mann-Whitney U test
Syt1$^{+/+}$ Internal Control WT	Syt1$^{+/+}$ Syt1^{WT}	P = 0.869	Mann-Whitney U test
Syt1$^{+/+}$ Internal Control F349A	Syt1$^{+/+}$ Syt1^{F349A}	P = 0.564	Mann-Whitney U test

Figure S2C anti-Myc Ab

Condition 1	Condition 2	P value	Statistical test
Syt1$^{+/+}$ Control	Syt1$^{+/+}$ Syt1^{WT}	P < 0.001	Mann-Whitney U test
Syt1$^{+/+}$ Control	Syt1$^{+/+}$ Syt1^{F349A}	P < 0.001	Mann-Whitney U test
Syt1$^{+/+}$ Syt1^{WT}	Syt1$^{+/+}$ Syt1^{F349A}	P = 0.712	Mann-Whitney U test
Syt1$^{+/+}$ Internal Control WT	Syt1$^{+/+}$ Syt1^{WT}	P < 0.001	Mann-Whitney U test
Syt1$^{+/+}$ Internal Control F349A	Syt1$^{+/+}$ Syt1^{F349A}	P < 0.001	Mann-Whitney U test

Figure S3

Bafilomycin treatment

Condition	Number of imaged coverslips	Number of preparations
Syt1$^{-/-}$ Control / Bafilomycin	23	5
Syt1$^{+/+}$ Control / Bafilomycin	23	5

Figure S3B RRP size

Condition 1	Condition 2	P value	Statistical test
Syt1$^{-/-}$ Control	Syt1$^{-/-}$ Bafilomycin	P = 0.354	Paired t-test on Ranks
Syt1$^{+/+}$ Control	Syt1$^{+/+}$ Bafilomycin	P = 0.218	Paired t-test on Ranks

Figure S4

Sucrose experiment

Condition	Number of cells	Number of preparations
Syt1$^{-/-}$ Control	18	3
Syt1$^{+/+}$ Control	16	3

Figure S4B RRP size

Condition 1	Condition 2	P value	Statistical test
Syt1$^{+/+}$ Control	Syt1$^{-/-}$ Control	P = 0.076	Mann-Whitney U test

Figure S4B Capacitance

Condition 1	Condition 2	P value	Statistical test
Syt1$^{+/+}$ Control	Syt1$^{-/-}$ Control	P = 0.018	Mann-Whitney U test

Figure S4B Normalized RRP size

Condition 1	Condition 2	P value	Statistical test
Syt1$^{+/+}$ Control	Syt1$^{-/-}$ Control	P = 0.569	Mann-Whitney U test

Figure S4C

Excitatory synaptic density

Condition	Number of synaptic ROIs	Number of preparations
Syt1$^{-/-}$ Control	20	4
Syt1$^{+/+}$ Control	20	4

Figure S4C VGlut1 density at dendrites

Condition 1	Condition 2	P value	Statistical test
Syt1$^{+/+}$ Control	Syt1$^{-/-}$ Control	P = 0.679	Student t test

Figure S4D

Neuronal arborisation

Condition	Number of cells	Number of preparations
Syt1$^{-/-}$ Control	15	3
Syt1$^{+/+}$ Control	12	3

Two-way ANOVA on Ranks P < 0.01.

Figure S5

Figure S5B and 5F - Western Blot analysis

Condition	Number of preparations
Syt1$^{+/+}$ Control	4
Syt1$^{+/+}$ Syt7 KD	4
Syt1$^{+/+}$ Syt1^{WT}	3
Syt1$^{+/+}$ Syt1^{F349A}	4

Syt1$^{+/+}$ Syt1^{WT} Syt7 KD	3
Syt1$^{+/+}$ Syt1^{F349A} Syt7 KD	4

Figure S5B anti-Syt7 Ab

Condition 1	Condition 2	P value	Statistical test
Syt1$^{+/+}$ Control	Syt1$^{+/+}$ Syt7 KD	P = 0.049	Student t test

Figure S5B anti-Syt1 Ab

Condition 1	Condition 2	P value	Statistical test
Syt1$^{+/+}$ Control	Syt1$^{+/+}$ Syt7 KD	P = 0.661	Student t test

Figure S5F anti-Syt7 Ab

Condition 1	Condition 2	P value	Statistical test
Syt1$^{+/+}$ Syt1^{WT}	Syt1$^{+/+}$ Syt1^{WT} Syt7 KD	P = 0.007	Student t test
Syt1$^{+/+}$ Syt1^{F349A}	Syt1$^{+/+}$ Syt1^{F349A} Syt7 KD	P = 0.008	Student t test

Figure S5F anti-Syt1 Ab

Condition 1	Condition 2	P value	Statistical test
Syt1$^{+/+}$ Syt1^{WT}	Syt1$^{+/+}$ Syt1^{WT} Syt7 KD	P = 0.846	Student t test
Syt1$^{+/+}$ Syt1^{F349A}	Syt1$^{+/+}$ Syt1^{F349A} Syt7 KD	P = 0.407	Student t test

Figure S5D and 5H- Immunostaining

Condition	Number of cells ROIs	Number of preparations
Syt1$^{+/+}$ Control	25	5
Syt1$^{+/+}$ Syt7 KD Control	25	5
Syt1$^{+/+}$ Syt1^{WT}	15	3
Syt1$^{+/+}$ Syt1^{F349A}	12	3
Syt1$^{+/+}$ Syt1^{WT} Syt7 KD	12	3
Syt1$^{+/+}$ Syt1^{F349A} Syt7 KD	12	3

Figure S5D anti-mCherry Ab

Condition 1	Condition 2	P value	Statistical test
Syt1$^{+/+}$ Control	Syt1$^{+/+}$ Syt7 KD Control	P < 0.001	Mann-Whitney U test

Figure S5D anti-Syt7 Ab

Condition 1	Condition 2	P value	Statistical test
Syt1$^{+/+}$ Control	Syt1$^{+/+}$ Syt7 KD Control	P = 0.001	Mann-Whitney U test

Figure S5H anti-Myc Ab

Condition 1	Condition 2	P value	Statistical test
Syt1$^{+/+}$ Syt1^{WT}	Syt1$^{+/+}$ Syt1^{WT} Syt7 KD	P = 0.903	Mann-Whitney U test
Syt1$^{+/+}$ Syt1^{F349A}	Syt1$^{+/+}$ Syt1^{F349A} Syt7 KD	P = 0.931	Mann-Whitney U test

Figure S5H anti-Syt7 Ab

Condition 1	Condition 2	P value	Statistical test
Syt1$^{+/+}$ Syt1^{WT}	Syt1$^{+/+}$ Syt1^{WT} Syt7 KD	P < 0.001	Mann-Whitney U test
Syt1$^{+/+}$ Syt1^{F349A}	Syt1$^{+/+}$ Syt1^{F349A} Syt7 KD	P < 0.001	Mann-Whitney U test

Supplementary References

1. Ariel P & Ryan TA (2010) Optical mapping of release properties in synapses. Front Neural Circuits. 4(.

2. Bacaj T et al. (2015) Synaptotagmin-1 and -7 Are Redundantly Essential for Maintaining the Capacity of the Readily-Releasable Pool of Synaptic Vesicles. PLoS.Biol. 13(10):e1002267.

3. Chanaday NL & Kavalali ET (2018) Optical detection of three modes of endocytosis at hippocampal synapses. Elife. 7. pii: 36097. doi: 10.7554/eLife.36097.(:36097.

4. Chang S, Trimbuch T, & Rosenmund C (2018) Synaptotagmin-1 drives synchronous Ca(2+)-triggered fusion by C2B-domain-mediated synaptic-vesicle-membrane attachment. Nat.Neurosci. 21(1):33-40.

5. Geppert M et al. (1994) Synaptotagmin I: a major Ca2+ sensor for transmitter release at a central synapse. Cell. 79(4):717-727.

6. Kaeser PS & Regehr WG (2017) The readily releasable pool of synaptic vesicles. Curr.Opin.Neurobiol. 43:63-70. doi: 10.1016/j.conb.2016.12.012. Epub;%2017 Jan 16.(:63-70.

7. Kochubey O, Babai N, & Schneggenburger R (2016) A Synaptotagmin Isoform Switch during the Development of an Identified CNS Synapse. Neuron. 90(5):984-999.

8. Liu H, Dean C, Arthur CP, Dong M, & Chapman ER (2009) Autapses and networks of hippocampal neurons exhibit distinct synaptic transmission phenotypes in the absence of synaptotagmin I. J.Neurosci. 29(23):7395-7403.

9. Rosenmund C & Stevens CF (1996) Definition of the readily releasable pool of vesicles at hippocampal synapses. Neuron. 16(6):1197-1207.

10. Rothman JE, Krishnakumar SS, Grushin K, & Pincet F (2017) Hypothesis - buttressed rings assemble, clamp, and release SNAREpins for synaptic transmission. FEBS Lett. 591(21):3459-3480.

11. Soykan T et al. (2017) Synaptic Vesicle Endocytosis Occurs on Multiple Timescales and Is Mediated by Formin-Dependent Actin Assembly. Neuron. 93(4):854-866.

12. Stevens CF & Williams JH (2007) Discharge of the readily releasable pool with action potentials at hippocampal synapses. J.Neurophysiol. 98(6):3221-3229.

13. Sudhof TC (2013) Neurotransmitter release: the last millisecond in the life of a synaptic vesicle. Neuron. 80(3):675-690.

14. Sudhof TC & Rothman JE (2009) Membrane fusion: grappling with SNARE and SM proteins. Science. 323(5913):474-477.

15. Watanabe S et al. (2013) Ultrafast endocytosis at mouse hippocampal synapses. Nature 504(7479):242-247.

16. Xu J, Pang ZP, Shin OH, & Sudhof TC (2009) Synaptotagmin-1 functions as a Ca2+ sensor for spontaneous release. Nat.Neurosci. 12(6):759-766.

17. Zhou Q et al. (2017) The primed SNARE-complexin-synaptotagmin complex for neuronal exocytosis. Nature. 548(7668):420-425.